JOURNAL OF PHYSICAL ORGANIC CHEMISTRY
J. Phys. Org. Chem. 2007; **20:** 448–453
Published online 17 April 2007 in Wiley InterScience
(www.interscience.wiley.com) DOI: 10.1002/poc.1175

Cation sitting in aromatic cages: *ab initio* computational studies on tetramethylammonium–(benzene)$_n$ (n=3–4) complexes

Jiagao Cheng,[1,2,3] Zhen Gong,[2] Weiliang Zhu,[1,2]* Yun Tang,[3] Weihua Li,[3] Zhong Li[3] and Hualiang Jiang[2,3]*

[1]School of Science, East China University of Science and Technology, 130 Meilong Road, Shanghai 200237, China
[2]Drug Discovery and Design Center, Shanghai Institute of Materia Medica, Chinese Academy of Sciences, 555 Zuchongzhi Road, Shanghai 201203, China
[3]School of Pharmacy, East China University of Science and Technology, 130 Meilong Road, Shanghai 200237, China

Received 2 November 2006; revised 4 February 2007; accepted 9 February 2007

ABSTRACT: Quantum chemistry study was performed on interaction between tetramethylammonium (TMA) and aromatic cages by means of the MP2 method to show how TMA sits in an aromatic cage that is composed of benzenes. The MP2 calculations on TMA–(benzene)$_n$ complexes demonstrate that the more the benzene molecules in the aromatic cage, the stronger the binding strength between the cage and TMA. In details, the structure of TMA–(benzene)$_n$ ($n = 1$–4) complexes can be easily constructed by superimposing n TMA-benzene complexes via TMA, and the binding energies of the TMA–(benzene)$_n$ complexes are the sum of the n corresponding TMA-benzene systems. For instance, the distances between the N of TMA and the plane of the benzene ring are 4.238, 4.252, 4.264 ,and 4.276 Å, respectively, for TMA–(benzene)$_n$ ($n = 1$–4) complexes, and the BSSE corrected binding energies at MP2/6-311++G** level are −8.8, −17.3, −25.8 and −34.3 kcal/mol, respectively, for TMA–(benzene)$_n$ ($n = 1$–4) complexes. Thus, this study provides us useful information on how a cation interacts with an aromatic cage in terms of complex geometry and binding strength. Copyright © 2007 John Wiley & Sons, Ltd.

KEYWORDS: cation–π interaction; nocovalent intreraction; tetramethylammonium; morokuma decomposition analysis

INTRODUCTION

The interactions between cations and aromatic rings are generally viewed as cation–π interaction,[1–2] which plays an important role in the binding of proteins and their ligands at the binding site.[3–7] Energetically, a cation–π interaction is comparable to a typical hydrogen bond, and in some cases the interaction is even stronger than a typical salt bridge.[8] In the X-ray structure of *Torpedo californa* AChE (TcAChE), the interaction between ACh and Trp84 provides one of the best-documented examples of cation–π interaction in ligand-receptor recognition.[9,10] Meanwhile, protein crystal structures demonstrate that a cation is capable of binding with 3 or 4 aromatic residues.[11–20] For example, there are three tryptophan residues in the X-ray structure of the periplasmic ligand binding protein ProX (PDB code 1R9L)[11] interacting simultaneously with the positively charged quaternary amine of the ligand glycine betaine via three of the indole groups of the residues. Similar cation–π interaction between a cation and three aromatic residues, has also been found in the X-ray structure of a choline-binding domain in LytA (PDB code 1HCX).[12] Aleshin *et al.*, found that the protonated Lys108 in the crystal structure of glucoamylase is surrounded by two tryptophans and two tyrosines, an example of the interaction of a cation with as many as four aromatic rings.[13] The X-ray structure of the K^+ channel shows that the mouth of the extracellular entrance is composed of four aromatic rings from four of the conserved tyrosines.[14–17] Electrophysiological data suggest that the mechanism of blocking of the channel by quaternary ammonium moieties involves the interaction of the cationic moieties with the four phenol groups.[18–20] All these structural and functional data show a fact that a single cation can interact with one, two, three, or as many as four aromatic rings. In other words, a cation may stably sit in a cage composed of several aromatic systems.

However, little research has been devoted to the interaction of a cation with multi–π systems, relative to the extensive studies performed for the simpler cation–π interaction.[21–32] Certain critical issues need to be

**Correspondence to:* Prof. W. Zhu or H. Jiang, Drug Discovery and Design Center, Shanghai Institute of Materia Medica, Chinese Academy of Sciences, 555 Zuchongzhi Road, Shanghai 201203, China.
E-mails: wlzhu@mail.shcnc.ac.cn; hljiang@mail.shcnc.ac.cn

addressed, such as, whether the interaction of a cation with multi–π systems possesses characteristics similar to 1:1 cation–π systems. Previously, we carried out a theoretical study on several π–cation–π sandwiches, and found additivities of both structural and energetic parameters as comparing with simple cation–π systems.[21] Then, could these conclusions be extended to the interaction of a cation with three or with four π systems? How can the binding strength of a cation with an aromatic cage be estimated? Here we reported our computational study results on complexes TMA–(benzene)$_n$ ($n = 1$–4), to answer these questions.

COMPUTATIONAL DETAILS

In the present study, tetramethylammonium (TMA) cation was used to represent the cationic group found in the crystal structures of PDB, and benzene was used to mimic aromatic system. The initial structures of the complexes of a TMA with one, two, three, and four benzenes were designed and shown in Figures 1a, 1b, 1c, and 1d, respectively, to mimic the interaction modes in protein crystal structures. All the TMA–(benzene)$_n$ ($n = 1$–4)complexes, free TMA and benzene were fully optimized at MP2/6-31G* level. Frequency calculations at the same level were then carried out for each optimized structure to see whether they are true minimum energy structures on the potential surfaces. The binding energies, ΔE, were calculated at the MP2/6-311++G**//MP2/6-31G* level using the equation below.[33]

$$\Delta E = E_{\mathrm{TMA}-(\mathrm{benzene})n} - E_{\mathrm{TMA}} - n \times E_{\mathrm{benzene}}$$

It was then corrected by both the basis set superposition error (BSSE) and the zero-point energy (ZPE)

$$\Delta E^{corr} = \Delta E + \mathrm{BSSE} + \Delta\mathrm{ZPE}$$

The BSSE was estimated by using the equation

$$BSSE = \{E_{\mathrm{TMA}} - E_{\mathrm{TMA}-[(\mathrm{benzene})n]}\} + \{E_{(\mathrm{benzene})n} - E_{[\mathrm{TMA}]-(\mathrm{benzene})n}\}$$

Where $E_{TMA-[(benzene)n]}$ (or $E_{[\mathrm{TMA}]-(\mathrm{benzene})n}$) is the energy of fragment TMA (or benzene system), based on the geometry extracted from the optimized structure, with its own basis set augmented by the basis set of benzene system (or TMA). E_{TMA} (or ($E_{(\mathrm{benzene})n}$) is the energy of isolated fragment TMA (or benzene system), with just its own basis set. The ZPE was estimated at the MP2/6-31G* level. The calculation was performed using Gaussian03 software.[34]

Morokuma decomposition analysis[35] on binding energy was carried out at the HF/6-31G*//MP2/6-31G* level by using the software GAMESS[36] on Pentium IV PCs, to investigate the factors affecting the binding between TMA and benzene systems.

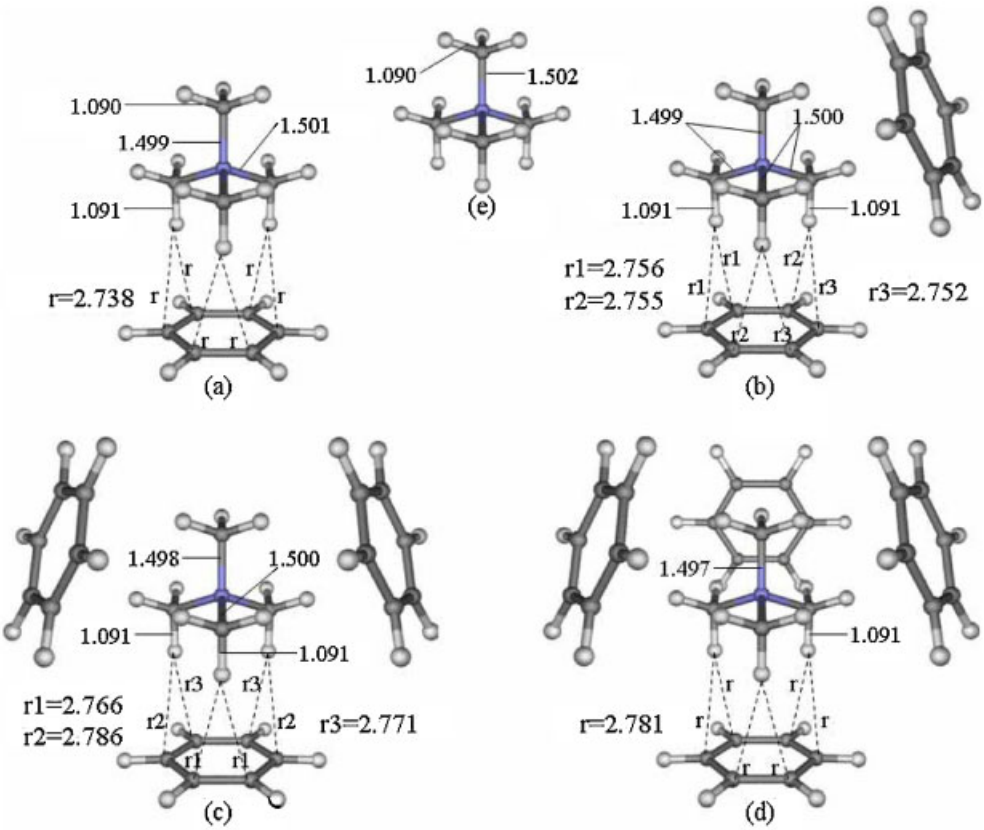

Figure 1. Optimized structures of TMA–(benzene)$_n$ ($n = 1$–4) complexes and free TMA monomer (distances in Å). This figure is available in colour online at www.interscience.wiley.com/journal/poc

DOI: 10.1002/poc

RESULTS AND DISCUSSION

Additivity in complex geometry

All the optimized TMA–(benzene)$_n$ ($n = 1$–4) complexes and free TMA structures at the MP2/6-31G* level were depicted in Fig. 1, which possess the same symmetries as in their initial structures. The vibrational frequency analysis at the same level gave no imaginary frequencies, suggesting that all the optimized structures are true energy minimum structures. The interaction between TMA and each benzene ring in TMA–(benzene)$_n$ ($n = 1$–4) is accomplished principally via three of its hydrogen atoms, each from one of the three methyl groups of TMA, very similar to that in TMA–benzene structure.

Figure 1 also provides the geometry parameters of the optimized structures. Comparing with free TMA, cation-π complexation leads to a slight contraction of the TMA C—N bonds and a slight elongation of the TMA C—H bonds. For example in TMA–(benzene)$_4$ complex, the C—N bond length decreases by 0.005 Å, while the C—H bond length increases by 0.001 Å. Table 1 summarizes the calculated perpendicular interaction distances between TMA and the benzene rings in the complexes. At MP2/6-31G* level, the distances between the N of TMA and the plane of the benzene ring are 4.238, 4.252, 4.264, and 4.276 Å for TMA–(benzene)$_n$ ($n = 1$–4) complexes, respectively. The distances are very similar in all TMA–(benzene)$_n$ ($n = 1$–4) complexes, and are elongated by less than 0.04 Å in TMA–(benzene)$_n$ ($n = 2$–4) complexes relative to the values in the TMA-benzene complex.

No other significant geometrical differences were observed. Thus, the structural unit of TMA–(benzene)$_n$ ($n = 2$–4) complexes is also the TMA–benzene complex, suggesting an additivity in the complex geometry of TMA with 2, 3 or 4 aromatic rings. In other words, the structure of TMA–(benzene)$_n$ ($n = 2$–4) complexes can be derived by adding benzene in a tetrahedral fashion taking advantage of the C—H interaction. For TMA–(benzene)$_4$ complex, the four benzene molecule just like the four plane of a tetrahedron around TMA.

Additivity in binding strength

The calculated energetic parameters at different levels were summarized in Table 2. At MP2/6-311++G** level, the BSSE and ΔZPE corrected binding energies, ΔE^{corr}, are −8.2, −16.1, −24.2 and −32.2 kcal/mol, respectively for TMA–(benzene)$_n$ ($n = 1$–4) complexes. Clearly, the binding energy between TMA and the aromatic cage of the TMA–(benzene)$_n$ ($n = 2$–4) complexes could be easily estimated as the sum of the binding energies of n corresponding TMA-benzene systems, indicating an additivity in binding strength, which is similar to the previous findings in π–TMA–π sandwiches.[21] To further illustrate the linear proportion, the energy values at MP2/6-311++G** level were plotted versus the number of benzene ring in the aromatic cage. Regression analysis revealed correlation coefficients (R^2) of 1.0000 and 1.0000 for ΔE and ΔE^{corr}, respectively, demonstrating a perfect linear correlation between binding strength and the number of the aromatic rings.

The calculated BSSE values at MP2 level are quite large relative to whole binding energies. At MP2/6-311++G** level, the percentage of BSSE over ΔE^{corr} are 36.6%, 38.5%, 39.3% and as high as 40.4%, respectively, for TMA–(benzene)$_n$ ($n = 1$–4) complexes (Table 2). Similar to our previous studies,[21–23] correction of BSSE is essential for TMA–(benzene)$_n$ ($n = 1$–4) complexes. Furthermore, Table 2 reflects another additivity that the BSSE values for the TMA–(benzene)$_n$ ($n = 2$–4) complexes are the sum of BSSE for n stand-alone TMA–benzene complexes. At MP2/6-311++G** level, the correlation coefficient (R^2) values between the BSSEs and n are 0.9991 for TMA–(benzene)$_n$ ($n = 1$–4) complexes. In comparison with the MP2 BSSE, the BSSE values calculated by B3LYP/6-311++G**//MP2/6-31G* and HF/6-311++G**// MP2/6-31G* methods are quite small, which are less than 2.5 kcal/mol in all complexes.

The ZPE corrections for the MP2 binding energy were performed at MP2/6-31G* level, which is quite small in comparison with the overall binding energy and with the MP2 BSSE correction. It ranges from 0.6 to 2.1 kcal/mol for TMA–(benzene)$_n$ ($n = 1$–4) complexes. Interestingly, the linear proportion property in ΔZPE also exists. At the MP2/6-31G* level, the correlation coefficient (R^2) values between the ΔZPE and the number of benzene ring (n) are 0.9942.

It is recognized that the HF theory does not take into account the electron correlation, and that the B3LYP version of DFT method cannot deal properly with the dispersion interaction.[37–39] Thus, the difference in ΔE^{BSSE} between the HF and MP2 methods could be roughly viewed as the contribution of the electron correlation (E_{e-c}),[37] whereas the difference between the B3LYP and MP2 methods can be approximately regarded

Table 1. Calculated distances (in Å) from the N atom of TMA to the plane of benzene at the MP2/6-31G* level

Complex	TMA-benzene	TMA-(benzene)$_2$	TMA-(benzene)$_3$	TMA-(benzene)$_4$
Distance	4.238	4.252	4.264	4.276

DOI: 10.1002/poc

Table 2. Calculated energy parameters (kcal/mol) for TMA–(benzene)$_n$ ($n = 1$–4) complexes based on the MP2/6-31G* optimized structures

(a) At the MP2 level

	Basis set	Absolute energy	ΔE	BSSE	ΔE^{BSSEa}	ΔZPE	ΔE^{corrb}
TMA-(benzene)$_1$	6-31G*	−444.8499560	−11.1	2.7	−8.4	0.6	−7.8
	6-311++G**	−445.1450768	−11.8	3.0	−8.8	—	−8.2
TMA-(benzene)$_2$	6-31G*	−676.3242113	−21.5	5.2	−16.3	1.2	−15.1
	6-311++G**	−676.7479699	−23.5	6.2	−17.3	—	−16.1
TMA-(benzene)$_3$	6-31G*	−907.7974907	−31.2	7.5	−23.7	1.6	−22.1
	6-311++G**	−908.3509856	−35.3	9.5	−25.8	—	−24.2
TMA-(benzene)$_4$	6-31G*	−1139.2699080	−40.4	9.8	−30.6	2.1	−28.5
	6-311++G**	−1139.9542339	−47.3	13.0	−34.3	—	−32.2

(b) At the HF/6-311++G**//MP2/6-31G* level

	Absolute energy	ΔE	BSSE	ΔE^{BSSEa}	$E_{\text{e-c}}$[c]	$E_{\text{e-c}}$%[d]
TMA-(benzene)$_1$	−443.5034039	−3.7	0.5	−3.2	−5.6	63.6
TMA-(benzene)$_2$	−674.2639407	−6.9	1.1	−5.8	−11.5	66.5
TMA-(benzene)$_3$	−905.0235618	−9.4	1.6	−7.8	−18.0	69.8
TMA-(benzene)$_4$	−1135.7822366	−11.3	2.2	−9.1	−25.2	73.5

(c) At the B3LYP/6-311++G**//MP2/6-31G* level

	Absolute Energy	ΔE	BSSE	ΔE^{BSSEa}	E_{disp}[e]	E_{disp}%[f]
TMA-(benzene)$_1$	−446.5429215	−5.3	0.6	−4.7	−4.1	46.6
TMA-(benzene)$_2$	−678.8611969	−9.7	1.1	−8.6	−8.7	50.3
TMA-(benzene)$_3$	−911.1785621	−13.5	1.8	−11.7	−14.1	54.7
TMA-(benzene)$_4$	−1143.4950231	−16.8	2.5	−14.3	−20.0	58.3

[a] BSSE- corrected binding energy.
[b] BSSE- and ZPE- corrected binding energy, ZPE predicted at MP2/6-31G* level.
[c] $E_{\text{e-c}}$ is the estimated electron correlation energy, the ΔE^{BSSE} difference between HF/6-311++G**//MP2/6-31G* and MP2/6-311++G**//MP2/6-31G* level.
[d] The percentage contribution of $E_{\text{e-c}}$ to ΔE^{BSSE} at MP2/6-311++G** level.
[e] E_{disp} is the estimated dispersion energy, the ΔE^{BSSE} difference between B3LYP/6-311++G**//MP2/6-31G* and MP2/6-311++G**//MP2/6-31G* level.
[f] The percentage contribution of E_{disp} to ΔE^{BSSE} at MP2/6-311++G** level.

as the contribution of the dispersion interaction (E_{disp}).[38,39] For TMA–(benzene)$_n$ ($n = 1$–4) complexes, the contribution of $E_{\text{e–c}}$ are −5.6, −11.5, −18.0, and −25.2 kcal/mol, respectively, and the contribution of E_{disp} are −4.1, −8.7, −14.1, and −20.0 kcal/mol respectively. At the MP2/6-311++G** level, the percentage contribution of $E_{\text{e–c}}$ to ΔE^{BSSE} are 63.6%, 66.5%, 69.8%, 73.5%, respectively for TMA–(benzene)$_n$ ($n = 1$–4) complexes, suggesting that electron correlation is the dominant component of the binding energy. Remarkably, dispersion interaction is the major part of the electron correlation (Table 2), therefore, play essential role in the binding. For TMA–(benzene)$_n$ ($n = 1$–4) complexes, the percentage contribution of E_{disp} to ΔE^{BSSE} are 46.6%, 50.3%, 54.7%, and 58.3% respectively. When the number of benzene rings increases, the percentage contribution of $E_{\text{e-c}}$ to ΔE^{BSSE} increases, so does the percentage contribution of E_{disp} to ΔE^{BSSE}. The more the benzene rings, the larger percentage contribution of electron correlation, and the larger percentage contribution of dispersion interaction. The reason of the trends is unclear.

Besides the very weak interaction among aromatics in the complexes, there might be two more causes for the existing of the additivity. First, the potential well along the interaction distance should be very flat. Indeed, a potential energy scan that we performed for the aromatic cage (benzene)$_4$ at the MP2/6-31G** level revealed a little difference of 0.4 kcal/mol as the distance (from the center of the cage to the benzene ring) varies from 4.276 Å to 10.276 Å. Second, the interaction distance is very similar among different systems (4.238 Å to 4.276 Å), leading to similar binding strength between the cation and each aromatic.

Charge transfer

The Mulliken, NPA[40] (natural population analysis), and ChelpG[41] (electrostatic potential charges from electrostatic potentials generalized) atomic charges were calculated at the MP2/6-31G* level using the MP2 density. Then a complex was divided into two parts: TMA and the aromatic aggregate. Table 3 summarized the calculated charges.

All the three types of atomic charges show that charge transfer from TMA to benzene takes place (Table 3), indicating that charge transfer is involved in the binding

DOI: 10.1002/poc

Table 3. Charge transfer among TMA and benzene (BZ) at the MP2/6-31G* level

		TMA-BZ	TMA-$(BZ)_2$	TMA-$(BZ)_3$	TMA-$BZ)_4$
Mulliken	TMA	0.928	0.866	0.812	0.764
	$(benzene)_n$[a]	0.072	0.134	0.188	0.236
	benzene[b]	0.072	0.067	0.063	0.059
NPA	TMA	0.978	0.960	0.944	0.931
	$(benzene)_n$[a]	0.022	0.040	0.056	0.069
	benzene[b]	0.022	0.020	0.019	0.017
ChelpG	TMA	0.845	0.715	0.602	0.503
	$(benzene)_n$[a]	0.155	0.285	0.398	0.497
	benzene[b]	0.155	0.143	0.133	0.124

[a] The total transferred atomic charges.
[b] the transferred atomic charges on each benzene.

of TMA to aromatic cage. Among the three types of atomic charges, ChelpG has the biggest value and NPA has the smallest. Although different algorithms release different values, the total transferred charge values increases when the number of benzene ring increases, while the amount of transferred charges on each benzene ring decreases slightly. Using the ChelpG charge as a reference, the total transferred charge values are 0.155, 0.285, 0.398, and 0.497, respectively, while the corresponding transferred charges on each benzene are 0.155, 0.143, 0.133, and 0.124, respectively, for TMA–$(benzene)_n$ ($n = 1$–4) complexes.

Energy decomposition analysis

A breakdown of the full molecular interaction energy into a number of components can offer insight into the fundamental nature of the interaction. One popular means of such decomposition is via an approach developed by Morokuma and his colleagues.[35] The studied complexes were divided into two parts: TMA and the aromatic aggregate, corresponding to monomer 1 and monomer 2 for decomposing the cation-π interaction using the software GAMESS.[36] Morokuma decomposition analysis was performed at the HF/6-31G* level, based on the MP2/6-31G* optimized structure. The calculated results were summarized in Table 4, in which the ES, EX, PL, CT, MIX, and ΔE denote electrostatic, exchange repulsion, polarization, charge transfer, high order coupling, and total binding energies, respectively. The EX, CT, MIX and ΔE values were corrected by BSSE estimated with the software GAMESS as well.

Table 4. Morokuma decomposition analysis on binding energy at the HF/6-31G*//MP2/6-31G* after BSSE correction (kcal/mol)

	ΔE	ES	EX	PL	CT	MIX
TMA-$(benzene)_1$	−4.7	−7.3	6.6	−1.8	−3.2	1.0
TMA-$(benzene)_2$	−8.9	−14.0	12.5	−3.4	−6.2	2.2
TMA-$(benzene)_3$	−12.7	−20.3	17.9	−4.8	−8.9	3.4
TMA-$(benzene)_4$	−16.1	−26.4	22.9	−5.9	−11.4	4.8

Table 4 shows that ES, CT, and PL are always favorable to the binding between TMA and benzene aggregates. In all cases, the ES is the most important binding component; the CT and the PL make smaller contributions as well. The CT component tends to be larger in magnitude than the PL in all cases. On the other hand, Table 4 shows that exchange repulsion and high order coupling are always unfavorable to the binding between TMA and aromatics. The main obstacle to the binding comes from exchange repulsion, according to the decomposition results.

CONCLUSIONS

In conclusion, our study on TMA–$(benzene)_n$ ($n = 1$–4) complexes revealed a cation could stably sit in an aromatic cage. The more the cage has aromatic monomers, the stronger the binding strength between the aromatic cage and the cation. In details, additivities of both the geometries and the binding energies were observed through this study. The preferred structure of a TMA–$(benzene)_n$ ($n = 2$–4) complexes can be obtained by adding benzene in a tetrahedral fashion taking advantage of the C—H interaction. The binding energies of the TMA–$(benzene)_n$ complex are the sum of n number of TMA–benzene systems. The contribution of electron correlation to the overall binding energy was estimated to be at least 63.6%, with dispersion serving as the main component of the electron correlation interaction. Charge transfer takes place when TMA binding to the benzene aggregate. Energy decomposition analysis shows that the electrostatic, charge transfer and polarity always impel the binding between TMA and the aromatic cage, whereas the exchange repulsion and high order coupling always hamper the binding. Our result not only demonstrates that it is energetically favorable a cation sitting in an aromatic cage, but also provide an easy and accurate way to evaluate the binding between a cationic ligand and an aromatic cage in protein.

Acknowledgements

The authors gratefully acknowledge financial support from National Natural Science Foundation (Grant No. 20572117), the National Key R&D Program (Grant No. 2005BA711A04), and the Shanghai Postdoctoral Scientific Program. All the calculations were performed on the supercomputer at Shanghai Supercomputer Center.

REFERENCES

1. Dougherty DA. *Science* 1996; **271**: 163–168.
2. Ma JC, Dougherty DA. *Chem. Rev.* 1997; **97**: 1303–1324.

DOI: 10.1002/poc

3. Zacharias N, Dougherty DA. *Trends. Pharmcol. Sci.* 2002; **23**: 281–287.
4. Scrutton NS, Raine ARC. *Biochem. J.* 1996; **319**: 1–8.
5. Schmitt JD, Sharples CGV, Caldwell WS. *J. Med. Chem.* 1999; **42**: 3066–3074.
6. Brejc K, Dijk WJV, Klaassen RV, Schuurmans M, Oost JVD, Smit AB, Sixma TK. *Nature* 2001; **411**: 269–276.
7. Zarić S, Popović DM, Knapp EW. *Chem. Eur. J.* 2000; **6**: 3935–3942.
8. Gallivan JP, Dougherty DA. *J. Am. Chem. Soc.* 2000; **122**: 874–880.
9. Sussman JL, Harel M, Frolow F, Oefner C, Goldman A, Toker L, Silman I. *Science* 1991; **253**: 872–879.
10. Harel M, Schalk I, Ehret-Sabatier L, Bouet F, Goeldner M, Hirth C, Axelsen PH, Silman I, Sussman JL. *Proc. Natl. Acad. Sci. USA* 1993; **90**: 9031–9035.
11. Schiefner A, Breed J, Bosser L, Kneip S, Gade J, Holtmann G, Diederichs K, Welte W, Bremer E. *J. Bio. Chem.* 2004; **279**: 5588–5596.
12. Fernández-Tornero C, López R, García E, Giménez-Gallego G, Romero A. *Nature Struct. Biol.* 2001; **8**: 1020–1024.
13. Aleshin AE, Firsov LM, Honzatko RB. *J. Bio. Chem.* 1994; **269**: 15631–15639.
14. Doyle DA, Cabral JM, Pfuetzner RA, Kuo A, Gulbis JM, Cohen LS, Chait BT, MacKinnon R. *Science* 1998; **280**: 69–77.
15. MacKinnon R, Cohen LS, Kuo A, Lee A, Chait BT. *Science* 1998; **280**: 106–109.
16. Nakamura RL, Anderson JA, Gaber RF. *J. Bio. Chem.* 1997; **272**: 1011–1018.
17. Cooper EC, Jan LY. *Proc. Natl. Acad. Sci. USA* 1999; **96**: 4759–4766.
18. Luzhkow VB, Åqvist J. *FEBS Lett.* 2001; **495**: 191–196.
19. Roux B, MacKinnon R. *Science* 1999; **285**: 100–102.
20. Jarolimek W, Soman KV, Alam M, Brown AM. *Mol. Pharmacol.* 1996; **49**: 165–171.
21. Liu T, Zhu W, Gu J, Shen J, Luo X, Chen G, Puah CK, Silman I, Chen K, Sussman JL, Jiang H. *J. Phys. Chem. A* 2004; **108**: 9400–9405.
22. Zhu W, Tan X, Shen J, Luo X, Cheng F, Puah CM, Ji R, Chen K, Jiang H. *J. Phys. Chem. A* 2003; **107**: 2296–2303.
23. Zhu W, Luo X, Puah CM, Tan J, Shen J, Gu J, Chen K, Jiang H. *J. Phys. Chem. A* 2004; **108**: 4008–4018.
24. Hu J, Barbour L, Gokel GW. *Proc. Natl. Acad. Sci. USA* 2002; **99**: 5121–5126.
25. Gaberšček M, Mavri J. *Chem. Phys. Lett.* 1999; **308**: 421–427.
26. Bartoli S, Roelens S. *J. Am. Chem. Soc.* 2002; **124**: 8307–8315.
27. Kim D, Hu S, Tarakeshwar P, Kim KS, Lisy JM. *J. Phys. Chem. A* 2003; **107**: 1228–1238.
28. Yamada S, Misono T, Tsuzuki S. *J. Am. Chem. Soc.* 2004; **126**: 9862–9872.
29. Ruan C, Rodgers MT. *J. Am. Chem. Soc.* 2004; **126**: 14600–14610.
30. Biot C, Buisine E, Rooman M. *J. Am. Chem. Soc.* 2003; **125**: 13988–13994.
31. De Wall SL, Meadows ES, Barbour LJ, Gokel GW. *Proc. Natl. Acad. Sci. USA* 2000; **97**: 6271–6276.
32. Feller D, Dixon DA, Nicholas JB. *J. Phys. Chem. A* 2000; **104**: 11414.
33. Boys SF, Bernardi F. *Mol. Phys.* 1970; **19**: 553–556.
34. Frisch MJ, Trucks GW, Schlegel HB, Scuseria GE, Robb MA, Cheeseman JR, Montgomery JA Jr, Vreven T, Kudin KN, Burant JC, Millam JM, Iyengar SS, Tomasi J, Barone V, Mennucci B, Cossi M, Scalmani G, Rega N, Petersson GA, Nakatsuji H, Hada M, Ehara M, Toyota K, Fukuda R, Hasegawa J, Ishida M, Nakajima T, Honda Y, Kitao O, Nakai H, Klene M, Li X, Knox JE, Hratchian HP, Cross JB, Adamo C, Jaramillo J, Gomperts R, Stratmann RE, Yazyev O, Austin AJ, Cammi R, Pomelli CJ, Ochterski W, Ayala PY, Morokuma K, Voth GA, Salvador P, Dannenberg JJ, Zakrzewski VG, Dapprich S, Daniels AD, Strain MC, Farkas O, Malick DK, Rabuck AD, Raghavachari K, Foresman JB, Ortiz JV, Cui Q, Baboul AG, Clifford S, Cioslowski J, Stefanov BB, Liu G, Liashenko A, Piskorz P, Komaromi I, Martin RL, Fox DJ, Keith T, Al-Laham MA, Peng CY, Nanayakkara A, Challacombe M, Gill PMW, Johnson B, Chen W, Wong MW, Gonzalez C, Pople JA. *Gaussian 03, Revision C.02*, Gaussian: Inc., Wallingford CT, 2004.
35. Kitaura K, Morokuma K. *Int. J. Quantum Chem.* 1976; **10**: 325–340.
36. Schmidt MW, Baldridge KK, Boatz JA, Elbert ST, Gordon MS, Jensen JH, Koseki S, Matsunaga N, Nguyen KA, Su S, Windus TL, Cupuis M, Montgomery JA, Jr. *J. Comput. Chem.* 1993; **14**: 1347–1363.
37. Head–Gordon M, Pole JA, Frisch MJ. *Chem. Phys. Lett.* 1988; **153**: 503–506.
38. Kristyán S, Pulay P. *Chem. Phys. Lett.* 1994; **229**: 175–180.
39. Rappé AK, Bernstein ER. *J. Phys. Chem. A* 2000; **104**: 6117–6128.
40. Reed AE, Curtiss LA, Weinhold F. *Chem. Rev.* 1988; **88**: 899–926.
41. Breneman CM, Wiberg KB. *J. Comp. Chem.* 1990; **11**: 361–373.

DOI: 10.1002/poc